Journal of Polymer Research (2023) 30:41
https://doi.org/10.1007/s10965-022-03422-7

ORIGINAL PAPER

Tamarind/β-CD-g-poly (MAA) pH responsive hydrogels for controlled delivery of Capecitabine: fabrication, characterization, toxicological and pharmacokinetic evaluation

Umaira Rehman[1] · Rai Muhammad Sarfraz[1] · Asif Mahmood[2] · Tahir Mahmood[1] · Nighat Batool[1] · Bilal Haroon[1] · Yacine Benguerba[3]

Received: 1 September 2022 / Accepted: 15 December 2022 / Published online: 29 December 2022

Abstract
The present study was aimed for controlled delivery of capecitabine, an anticancer drug used to treat colorectal cancer. Smart pH responsive tamarind/-CD-g-poly (MAA) hydrogels were developed using the free radical polymerization process to overcome the constraints of capecitabine such as short plasma half-life, low bioavailability, and high dose frequency. The developed network system was evaluated for different characterizations including equilibrium swelling (%), drug loading efficiency (%), thermal behavior, elemental composition, morphology, complexation of components and release kinetics. Furthermore, safety profile of developed network was validated by acute oral toxicity studies and pharmacokinetic parameters were determined by carrying *in-vivo* studies in healthy rabbits. The grafted system proved to be thermally stable as confirmed by DSC and TGA analysis. While successful grafting, compatibility of hydrogel components and amorphous dispersion of drug within the network were shown by FTIR analysis and XRD studies. Significantly higher swelling and drug release were observed at pH 7.4 than at pH 1.2, evidencing pH responsive character of hydrogels. Maximum drug release of 94.3% was shown over period of 30 h demonstrating the controlled release profile of polymeric network. Toxicity evaluations revealed good safety profile and biocompatibility of hydrogels. Moreover, *in-vivo* studies showed sustained release profile of capecitabine as proved by significant increase in its half-life (13 h) and AUC (42.88 µg.h/ml) when administered as hydrogels. Hence, tamarind/β-CD-g-poly (MAA) hydrogels are strongly recommended to be employed as biocompatible pH responsive carrier system and can be utilized for controlled and targeted delivery of drugs.

Keywords Controlled delivery · pH responsive · Hydrogels · Pharmacokinetic · Half life

Introduction

Various approaches are being utilized in drug delivery to achieve the prolonged therapeutic response of active moieties with lesser side effects. Frequency of administration of most of the traditional dosage forms is high that is associated with side effects and may result in noncompliance behavior of patients. These problems can be overcome by use of certain techniques and systems that enhance the therapeutic response of active agents by delivering them

✉ Rai Muhammad Sarfraz
sarfrazrai85@gmail.com

Umaira Rehman
umairarehman@hotmail.com

Asif Mahmood
asif.mahmood@uoc.edu.pk

Tahir Mahmood
drtahirmahmood05@gmail.com

Nighat Batool
nighatbatool2352@gmail.com

Bilal Haroon
Bilal.haroon87@gmail.com

Yacine Benguerba
yacinebenguerba@univ-setif.dz

[1] Department of Pharmaceutics, College of Pharmacy, University of Sargodha, Sargodha, Pakistan

[2] Department of Pharmacy, University of Chakwal, Chakwal, Pakistan

[3] Laboratoire de Biopharmacie Et Pharmacotechnie (LBPT), Ferhat Abbas Setif 1 University, Setif, Algeria

slowly at controlled rate. So, these drug delivery systems result in improvement of bioavailability of therapeutic agents and reduction in frequency of administration and dose related side effects [1].

One of the appealing types of drug delivery system is hydrogels having extraordinary properties. Hydrogels are hydrophilic three-dimensional polymeric networks having capability to absorb excess of water or physiological fluid without experiencing any change in their geometry [2]. Hydrogels in swollen form resemble with living tissues due to their soft and rubbery consistency and low interfacial tension with water or biological fluids. These are non-irritant, non-toxic and biocompatible polymeric systems. Because of their intelligent properties, they show numerous advantages in drug delivery like protection of active moieties against GIT environment, site specific and sustained release of encapsulated drug [3, 4]. Physical and chemical cross-linking techniques are used for fabrication of hydrogels. Chemical gels are developed by covalent interactions and physical gels by non-covalent interactions [5]. They have numerous applications in medicines and clinical practice like tissue engineering and regenerative medicine, cellular immobilization, cells or biomolecules separation, diagnostics, and barrier materials for controlling biological adhesions. Presently, different forms of hydrogels have been developed like discs, microparticles [6], nanoparticles [7], coatings, matrixes [8], composites [9], slabs and films [10] depending upon the required use.

Tamarind gum is polysaccharide, a natural polymer obtained by extraction of *Tamarindus indica* seeds. It is hydrophilic polymer as its molecular structure contains numerous hydroxyl groups. It has ability to form mucilage by showing swelling behavior in water. Owing to its gel forming character it can also be employed in hydrogel development. The polymer is being used in pharmaceutical products due to its nontoxicity, biocompatibility and bioadhesive properties [11, 12].

Cyclodextrins belong to cyclic oligosaccharides having 1,4-linked glucopyranose units [13]. β-cyclodextrin (β-CD) is largely employed in pharmaceutical sector owing to its cavity size, ability to form complexes, easy availability and affordability. Keeping in view its excellent binding and complex forming characteristics it can incorporate numerous compounds (organic and inorganic) and therapeutic moieties within its cavity [14].

Miscibility of different polymers in development of hydrogels is a significant parameter. Florry and Huggins theory illustrate pharmacodynamic evaluation of polymeric blends using their molecular structure and binding energies of individual polymers. Moreover, binding energy curves also ensure level of miscibility i.e. whether miscible, partially miscible and immiscible [15–17].

Among numerous chemotherapeutic agents for cancer treatment Capecitabine is available as orally administered anticancer drug. It is a prodrug indicated for colorectal and metastatic breast cancers [18]. Capecitabine follows sequential enzymatic steps to convert into its final active metabolite that is 5-fluorouracil (5-FU) in the tumor, where it exerts its action. Half-life of drug is short i.e., 0.5–1 h. The recommended daily dose is 1250 mg/m [2] twice daily and associated with various side effects including dermatitis, stomatitis, diarrhea, bone marrow depression, cardiotoxicity, nausea, vomiting etc. High dosing frequency and adverse effects of drug are mostly reasonable factors of patient non-compliance behavior. So, there is need to synthesize the controlled release system having potential to enhance the bioavailability and minimize the toxic effects of Capecitabine that would also improve the patient compliance [19]. In literature, efforts have been made to incorporate capecitabine into different types of hydrogels i.e., hydrogel microspheres [20], interpenetrating polymeric networks [21] and nanocomposite hydrogels [19]. In comparison to these studies, promising results in terms of *in-vivo* release, pK parameters and *in-vitro* release were reported in our current study.

Oral route always remained a preferred route for delivery of therapeutic agents but, often offer inadequate bioavailability. A number of polymers have been tried in literature to develop hydrogels. In current study, pH responsive tamarind/β-CD-g- poly (MAA) hydrogels have been synthesized by using varying proportions of polymers, monomer, and crosslinking agent utilizing aqueous free radical polymerization technique in order to improve oral bioavailability of Capecitabine. Study is aimed to attain targeted and controlled release profile of Capecitabine by incorporating it into polymeric network that will reduce its dosing frequency thereby improving the patient compliance. Developed networks were subjected various instrumental evaluation techniques like compatibility studies (FTIR), thermal analysis (DSC, TGA), elemental analysis (EDX), surface morphology (SEM), nature of ingredients (PXRD), sol–gel analysis, pharmacokinetic evaluation and acute oral toxicity studies.

Materials and methods

Materials

Capecitabine was purchased from Wuhanvanz Pharma, Jingkai Future city Hubli, China. β -CD, methacrylic acid (99%), N, N-methylene bisacrylamide (99%), ammonium persulfate (99%), acetonitrile and methanol (99.7%) were purchased from Sigma-Aldrich Co., St Louis, MO, USA. Tamarind seed powder, Potassium dihydrogen phosphate, orthophosphoric acid, ethanol and sodium hydroxide were

purchased from Dae-Jung, Korea. Distilled water was prepared on daily basis in the research lab of the Faculty of Pharmacy, The University of Lahore. All the chemicals utilized were of analytical grade.

Methods

Extraction of tamarind seed mucilage

Tamarind seed polysaccharide was obtained by mucilage extraction of the seed powder. 20 g of tamarind seed powder was weighed and its slurry was prepared by adding it in 200 ml of cold distilled water. This slurry was transferred to 1L beaker containing 800 ml of boiling distilled water, placed on water bath and stirred continuously for 30 min at boiling temperature. After that it was set aside for approximately 24 h to sediment proteins and fibers. Mixture was then subjected to centrifugation for 20 min at 5000 rpm in order to collect the clear solution. This clear supernatant was transferred into double volume of absolute ethanol with thorough agitation to get thick precipitates. Resulting precipitates were washed with ethanol and kept in hot air oven at 40 °C for drying. After 24 h this dried polymer was triturated in pestle and mortar and passed through sieve assembly to get fine powder which was then stored in air tight container [22].

Development of tamarind gum/B-CD-g-poly (MAA) hydrogels

Tamarind gum/β-CD-g-poly (MAA) hydrogels were synthesized with variable contents of polymers, monomer and crosslinking agent using free radical polymerization technique. Composition of formulations (TGB1-TGB12) is presented in Table 1. Accurate quantity of β-CD was weighed on an electronic weighing balance (Shimadzu, AUW220D Japan), poured into specific volume of distilled water and stirred on hot plate magnetic stirrer until solution became clear. Then weighed amount of tamarind seed polysaccharide was dissolved in distilled water at room temperature separately. Solution of APS was prepared in small volume of distilled water separately and half of it was added in first polymer solution and half in second solution drop wise to generate active sites on polymer backbone with thorough stirring. Both polymer mixtures were mixed together thoroughly by addition of one polymer solution into other dropwise with continuous stirring. Monomer (MAA) was added in the above mixture followed by addition of crosslinker (MBA) with continuous mixing. Final volume of the mixture was achieved by adding deionized distilled water. System was subjected to thorough stirring until the formation of homogenous mixture and then transferred to glass tubes which were sonicated for 3 to 5 min to remove any dissolved oxygen. Glass tubes after covering with aluminium foil were placed in water bath (Memmert) and temperature was tuned sequentially which was 45 °C for 1 h, 50 °C for 2 h, 55 °C for 4 h, 60 °C for 6 h, and 65 °C for 12 h. Hydrogels formed after 24 h were removed by breaking the test tubes with back side of test tube holder and cut into discs which were washed with ethanol and distilled water solution (50:50) and dried in lyophilizer (Christ Alpha 1- 4 LD, Japan) at -55 °C [23].

Characterizations

Blend simulation studies

The Material Studio Blends module was used to study the β-cyclodextrin-g-poly(methacrylic acid) with tamarid miscibility. This approach enables researchers to get insight of the thermodynamics involved among different materials utilizing their chemical formulas. So, it only uses molecular

Table 1 Composition of Tamarind gum/β-CD-g-poly (MAA) hydrogels

Formulation code	Tamarind gum (g/100 g)	β -CD (g/100 g)	MAA (g/100 g)	MBA (g/100 g)	APS (g/100 g)
TGB1	0.5	0.25	10	0.2	0.2
TGB2	1	0.25	10	0.2	0.2
TGB3	1.5	0.25	10	0.2	0.2
TGB4	0.5	0.5	10	0.2	0.2
TGB5	0.5	0.75	10	0.2	0.2
TGB6	0.5	1	10	0.2	0.2
TGB7	0.5	0.25	14	0.2	0.2
TGB8	0.5	0.25	16	0.2	0.2
TGB9	0.5	0.25	18	0.2	0.2
TGB10	0.5	0.25	10	0.25	0.2
TGB11	0.5	0.25	10	0.3	0.2
TGB12	0.5	0.25	10	0.35	0.2

structures and an energy field as precursor input data for blend simulation.

Miscibility among mixture of different nature materials can be demonstrated via thermodynamic relationships. This approach is based on a theory developed by Flory and Huggins. It concludes by finding the free energies of the mixing thereby reflecting state of mixture and declare the materials are either miscible, immiscible, or partially miscible [15, 16], according to the following equation: n

$$\frac{\Delta G}{RT} = \frac{\varnothing_A}{n_A} ln\varnothing_A + \frac{\varnothing_B}{n_B} ln\varnothing_B + \chi\varnothing_A\varnothing_B \quad (1)$$

In which ΔG is the Free energy of mixing, K is the Boltzmann constant, T is the Absolute temperature, $\varnothing_A$ and $\varnothing_B$ are the volume fraction of A (Tamarind) and B (β-cyclodextrin-g-poly(methacrylic acid))components, n_A and n_B represent mole numbers of component A and B, respectively and χ is the of Flory Huggins parameter.

The parameter of Flory Huggins (χ) is defined as follows [17]:

$$\chi = \frac{E_{mix}}{RT} \quad (2)$$

The mixing energy, E_{mix}, can be calculated by using following expression that presents difference in free energy between the mixture and the sum of the pure energy of A and B [15, 16].

$$E_{mix} = \frac{1}{2} Z(E_{bs} + E_{sb} - E_{bb} - E_{ss}) \quad (3)$$

E_{bb} and E_{ss} are the binding energies between two base (tamarind) molecules and two screen (β-cyclodextrin-g-poly(methacrylic acid)) molecules in their pure states. E_{bs}, and E_{sb} are the binding energies between base and screen molecules. Z is the coordination number [16].

Loading of Capecitabine

Capecitabine was loaded into the weighed hydrogels dried disks. Briefly, 1% w/v solution of Capecitabine was prepared by adding 1 g of Capecitabine in a beaker containing specified volume of phosphate buffer solution (pH 7.4) and then stirred on hot plate magnetic stirrer at room temperature for approximately 30 min to obtain clear solution. Weighed hydrogel discs were soaked in it until swelled to equilibrium. These swollen discs were blotted with filter paper after removing from drug solution and dried in hot air oven (Memmert) at 45°C followed by drying at room temperature.

Quantification of Capecitabine

Percentage of drug loaded into hydrogels was calculated by using following equation: [24]

$$Drug\ loading(\%) = \frac{WD - Wd}{Wd} \times 100 \quad (4)$$

where, *WD* = final weight of dried discs of hydrogels after immersion in drug solution.

Wd = initial weight of dried hydrogel discs before immersion in drug solution.

In-vitro swelling studies

pH responsive behavior of hydrogels was evaluated by performing swelling experiments on hydrogels. Dried discs were precisely weighed on electric weighing balance (Shimadzu, AUW220D) and then placed in phosphate buffer solution (pH 7.4) at 37 °C. After specified time intervals (0.5, 1, 1.5, 2, 3, 4, 5, 6, 12, 18, 24, 30, 36, 42, and 48 h) swollen discs were removed from the solution, blotted with absorbent paper and weighed again. Experiment was continued until all discs achieved a constant weight. Following equation was used to calculate the percentage swelling of hydrogels [25].

$$\%\text{Swelling} = \frac{Wt - Wo}{Wo} \times 100 \quad (5)$$

where, *Wo* is the initial weight of dried disc and *Wt* is the weight of swollen disc at time t.

Sol–gel fraction

Sol–gel fraction was determined to find out the reactants utilized during synthesis of hydrogels. Dried discs were weighed on electronic weighing balance and crushed into small particles. Extraction was conducted in Soxhelt apparatus containing boiling distilled water for 4 h so that the co-polymeric network could be freed from unreacted reactants. Extracted hydrogel pieces were removed by using filter paper and dried at room temperature for 24 h followed by drying in hot air oven at 40 – 45 °C and these were reweighed [26].

Sol–gel fraction was calculated by using following formula:

$$Gel\ fraction(\%) = \frac{Wt}{Wo} \times 100 \quad (6)$$

where, Wo = Initial weight of dried disc before extraction and Wt = Final weight of dried disc after extraction.

Moreover, Sol fraction was calculated by following expression:

$$Sol\ fraction = 100 - gel\ fraction \quad (7)$$

Fourier transforms infrared spectroscopy

Pure Capecitabine, HP-β-CD, agarose, chitosan, fenugreek, tamarind, β-CD, physical mixture, drug loaded and unloaded hydrogels were subjected to FTIR analysis to check the complex formation and compatibility between ingredients. All the samples were grounded and dried after mixing with KBr, then 65 kN pressure was used for 1 min to convert into disc having 12 mm thickness. Scanning of these samples was done at 4000 to 500 cm^{-1} using Thermos Fischer scientific Nicolet 6700 TM) FTIR spectrophotometer [27].

Scanning electron microscopy

Scanning electron microscope (SEM, Vega 3, Tuscan) was used for evaluation of surface morphology and shape of prepared hydrogels. Dried hydrogels were crushed into small particles and attached to double adhesive tape on aluminum stub. Gold coating having thickness of 300 Å was done on aluminium stubs. Current of 10 kV was set for scanning of coated samples and recording of surface morphology [28, 29].

Differential scanning calorimetry

Drug, polymers, monomer and developed hydrogels were subjected to DSC studies in order to determine the phase transition temperatures and heat of fusion under rising temperature. Properly ground samples were covered in an aluminium pan. Operation of SDT (Q600 TA USA) was carried out at a rate of 10 °C/min under nitrogen stream using temperature range of 0–400 °C. Analysis was done in triplicate for each sample [30].

Thermogravimetric analysis (TGA)

Stability of newly developed polymeric network against individual formulation ingredients at elevated temperature was determined using TGA thermal analysis under the same conditions as in DSC.

Powder x-ray diffraction (PXRD) analysis

RXD Xpert having pan analytical software was used to confirm the nature i.e. amorphous or crystalline of pure Capecitabine, polymers and loaded hydrogels. Scanning was done at $2\theta = 10°\text{-}70°$. All samples were performed in triplicate [31].

Elemental dispersive x-ray spectroscopy

Elemental composition and atomic weight of components were determined using microanalysis technique which is energy dispersive spectroscopy. This technique was utilized by using INCA 200 m oxford, UK for developed hydrogels. Pure drug, unloaded and loaded hydrogels were subjected to energy dispersive spectroscopy and their spectra were recorded [32].

In- vitro drug release

In-vitro drug release studies were carried out to confirm the pH responsive release of Capecitabine from hydrogels at pH 1.2 and 7.4. USP dissolution apparatus Type-II containing 900 ml of buffer solution in each basket was used at 37 ± 0.5 °C to perform dissolution studies of hydrogel formulations. Sampling was done at specified intervals i.e. 0.5, 1, 1.5, 2, 3, 4, 6, 8, 10, 12, 14, 16, 18, 20, 22 and 24 h and UV visible spectrophotometer was used for analysis of Capecitabine at $\lambda_{max} = 300$ nm [33, 34].

Kinetic modeling for analysis of drug release pattern

Drug concentration, swelling and diffusion rate are the factors on which drug release from hydrogel cross-linked structure is dependent. Mechanism of capecitabine release from developed hydrogels was determined by applying kinetic models (Zero order, First order, Higuchi and Korsmeyer-Peppas) on release data through DD solver adds in option of Microsoft Excel. Values of n and R2 provided the mechanism of drug release and best fit model, respectively. Fickian diffusion was governed by value of "n" equal to 0.45, anomalous or non-fickian diffusion was shown by values ranging within 0.45–0.89 and case-II transport or zero order was proved by value equal to 0.89 [35].

Zero order kinetics

$$Ft = Fo - Kot \quad (8)$$

First-order kinetics

$$ln(1 - F) = -K_1 t \quad (9)$$

Higuchi model

$$Ft = K_H t^{1/2} \quad (10)$$

where, F_t = Fraction of drug release in time t, F_o = Total amount of Capecitabine in polymeric networks, Ko, $K1$ and K_H are the rate constants for Zero order, First order and Highuchi models, respectively.

Korsemeyer-Peppas model is described as

$$Ft = K_H t^{1/2} \quad (11)$$

Mt/M∞ shows portion of Capecitabine released at time t, K_3 is Rate constant and n describes release exponent.

Acute oral toxicity studies on animal model

To evaluate the effect of carrier system on biochemical, lipid and renal profile, vital organs and physical activity of rabbits, toxicity studies were conducted. Economic cooperation and development guidelines were strictly followed for this purpose. All the study protocols were reviewed and approved by Institutional Research Ethics Committee of Faculty of Pharmacy, The University of Lahore vide notification no. IREC-2020–25. Twelve healthy albino rabbits were taken by following OECD guidelines. They were acclimatized for 7 days in stainless steel cages and fed with proper diet and water. Rabbits were divided into two groups i.e. group A (control) and group B (tested) by keeping six rabbits in each group. After overnight fasting of group B hydrogels in crushed form (2 g/kg) were administered to it through feeding tube and both the groups were kept under observation for food consumption and water intake, body weight, skin allergies and any physical changes for 14 days. On 7th day, for collection of blood samples, ears of animals were cleaned off hairs by applying hair removing cream and 2-3 ml of blood sample was collected from marginal vein of ear by using 3 cc syringes (Injekt®) and transferred into EDTA tubes. These tubes were rotated between palms of the hands to prevent blood coagulation. Blood samples were subjected to centrifugation for 15 min (Hitachi Zentrifugen EBA 20, Hitachi Ltd., Tokyo, Japan) at 5000 rpm for hematological analysis, AST, ALT, lipid and renal profile. After 14 days, all rabbits were re-weighed and anesthetized by injecting combination of ketamine and xylazine (70:30) at a dose of 1 ml/kg into the thigh muscles of animals. Blood samples were withdrawn again by heart puncture and vital organs (heart, liver, kidney, lungs, intestine, stomach, spleen and brain) were removed and washed with tap water. These organs were than stored in labeled separate plastic jars containing 10% formalin solution and subjected to histopathological examination.

Pharmacokinetics study

Pharmacokinetic evaluation of capecitabine was carried out by conducting *in-vivo* studies adapting cross over study design. For this, eighteen healthy male rabbits (2–2.5 kg) were acclimatized for one week under 12/12-h light/dark cycle and divided into three groups (n = 6). Group A was kept as control and other two groups (B and C) were fasted overnight with free access to water. Oral powder of pure capecitabine was administered to group B at a dose of 10 mg/Kg. While group C was given equivalent dose of drug loaded hydrogels (10 mg/Kg) in crushed form encapsulated in hard gelatin capsules followed by 5-10 ml of water. At predetermined time intervals (0, 1, 2, 3, 4, 6, 8, 10, 12, 16, 20 and 24 h) 2-3 ml of blood samples were withdrawn from jugular vein and collected in EDTA tubes immediately. For separation of plasma all the samples were subjected to centrifugation for 15 min at 5000 rpm. Each sample was deproteinized by taking 1 ml of plasma in glass centrifuge tube, added equal volume of HPLC grade methanol and vortexed for 3 min. These tubes were centrifuged again at 5000 rpm for 15 min to separate the supernatant that was collected carefully by micropipette and diluted with mobile phase for analysis. After providing washout period of 2 weeks to animals, group B was administered with drug loaded hydrogels while oral powder of capecitabine was given to group C in similar dose. Experiment was repeated as described above. Analysis of Capecitabine in plasma samples was carried out by using a developed HPLC method with certain modifications [27]. Water and acetonitrile mixture (50:50 v/v) was used as mobile phase at flow rate of 1 ml/min. A reverse phase C18 column was used having dimensions of 250 mm 4.6 mm 5 µ. Capecitabine was detected by scanning at λmax of 310 nm after transferring the samples into autosampler vials. Different pharmacokinetic parameters (C_{max}, t_{max}, MRT, $t_{1/2}$, $AUC_{0\text{-}t}$, $AUMC_{0\text{-}inf}$ and Cl) were calculated by using noncompartmental analysis of pharmacokinetic model.

Results and discussion

The blend of the one interacting system i.e. β-cyclodextrin-g-poly(methacrylic acid) with tamarind was evaluated for miscibility. The results indicate sufficient mixing energy between β-cyclodextrin-g-poly(methacrylic acid) and tamarind (18.088 kcal mol^{-1} at 298 K with X = 30.54) as shown in Table 2. The Florry-Huggins parameter, χ shows that it is easier to mix β-cyclodextrin-g-poly(methacrylic acid) with tamarind. The calculated coordination number Z_{bb} indicates that 5.508 molecules of "b" molecule surround one "b" molecule. Likewise, coordination number Z_{bs} indicates that 6.09 molecules of "b" are surrounding one "s" molecule. Moreover, coordination number Z_{ss} indicate 5.52 molecules of "s" are distributed around one "s" molecule. These findings suggest higher miscibility and compatibility of these polymers. Grafted presentation of β-cyclodextrin-g-poly(methacrylic acid) with tamarind is shown in Fig. 1A.

Based on binding energy curves as shown in Fig. 1B, it is evident that Ess, Ebs and Ebb curves are superposed each other that warrant perfect miscibility of these polymers. While compatible structure of developed tamarind gum/β-CD-g- poly (MAA) hydrogel is shown in Fig. 1A.

In literature a number of investigations have been performed where miscibility of polymeric blend confirmed

Table 2 Blend of one interacting system containing Tamarind and β-cyclodextrin-g-poly(methacrylic acid) blend's module: Energies are in kcal mol^{-1}

Base (b)	Tamarind
Screen (s)	β-cyclodextrin-g-poly(methacrylic acid)
χ (298 K)	30.54
E_{mix} (298 K)	18.088
Ebb avg	-16.889
Ebs avg	-13.878
Ess avg	-17.508
Zbb	5.508
Zbs	6.09
Zsb	4.97
Zss	5.52

through simulation approach working on Florry Huggins theory [36–39].

Drug loading (%)

Capecitabine was loaded as model drug into tamarind gum/ β-CD-g- poly (MAA) hydrogels. Pre-weighed dried discs of hydrogels were soaked in 100 ml of 1% w/v Capecitabine solution in phosphate buffer (pH 7.4) for 48 h and loading percentage was calculated after drying the discs. For all formulations (TGB1-TGB12), Capecitabine loading was ranged from 69.05% to 86.17% as presented in Fig. 2. It was markedly influenced by varying the proportions of polymers, monomer and crosslinking agent in grafted network. Drug loading percentage was increased by rising the tamarind gum (TGB1-TGB3), β-CD (TGB4-TGB6) and MAA (TGB7-TGB9) contents in formulations from 70.83% to 79.69%, 73.97% to 82.39% and 77.12% to 86.17%, respectively. While, decrease in drug loading was presented by formulations (TGB10-TGB12) having increased contents of MBA ranging within 78.1%-69.05%. Highest drug loading was exhibited by formulation (TGB9) showing maximum swelling response.

Swelling behavior

Swelling behavior of hydrogels was investigated by immersing the formulations in phosphate buffer solution (pH 7.4) till equilibrium was attained. Four batches of twelve formulations were prepared with varying concentrations of polymers (tamarind gum and β-CD), monomer (MAA) and crosslinking agent (MBA) and effect of these contents on swelling response was evaluated. All formulations retained their structure and shape during whole period. Results are displayed in Fig. 3.

An increase in equilibrium swelling was observed ranging from 82.45%-91.09% for formulations (TGB1-TGB3) containing variable quantities of tamarind gum. That enhanced swelling was attributed to electrostatic repulsion between functional groups of polymer at pH 7.4 giving rise to larger spaces available for intake of water molecules.

Sequential rising of β-CD in formulations TGB4-TGB6 also resulted in increased swelling response from 83.41%-92.50%. This effect can be explained in terms of hydrophilic character of β-CD enabling its greater functional units available to link with MAA resulting in expansion of the network. Similar swelling trends were observed at alkaline pH previously for β-CD hydrogels by a study conducted by Roy et al. [40]. Likewise, incremental rise of MAA in formulations TGB7-TGB9 promoted the

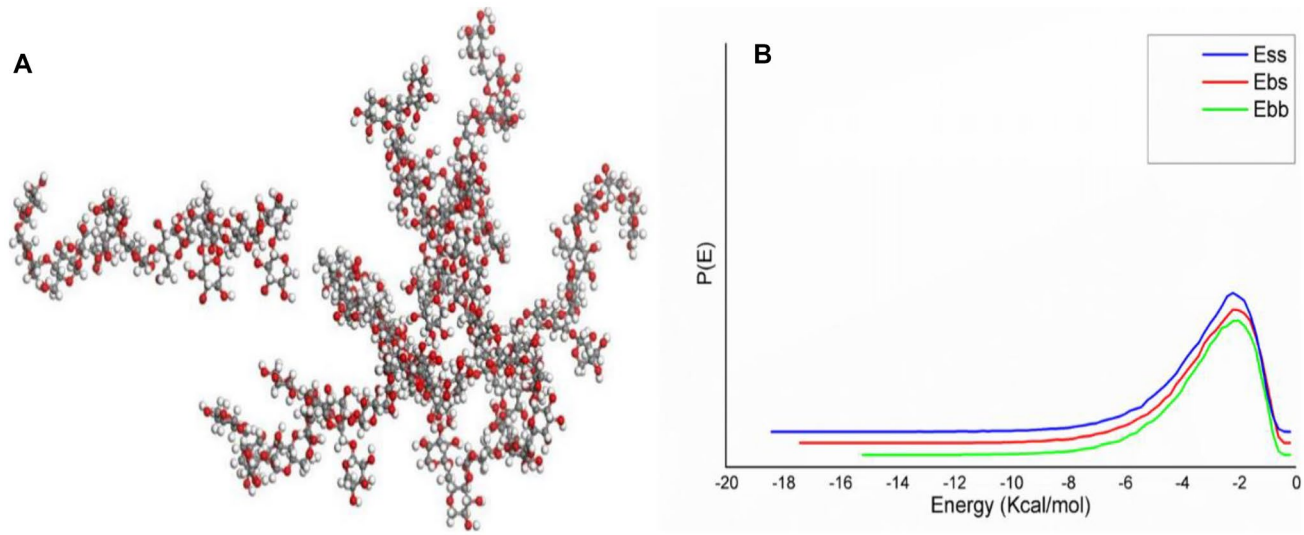

Fig. 1 **A** Structure of tamarind gum/ β-CD-g- poly (MAA) hydrogel and **B** Blend binding energy distribution curves

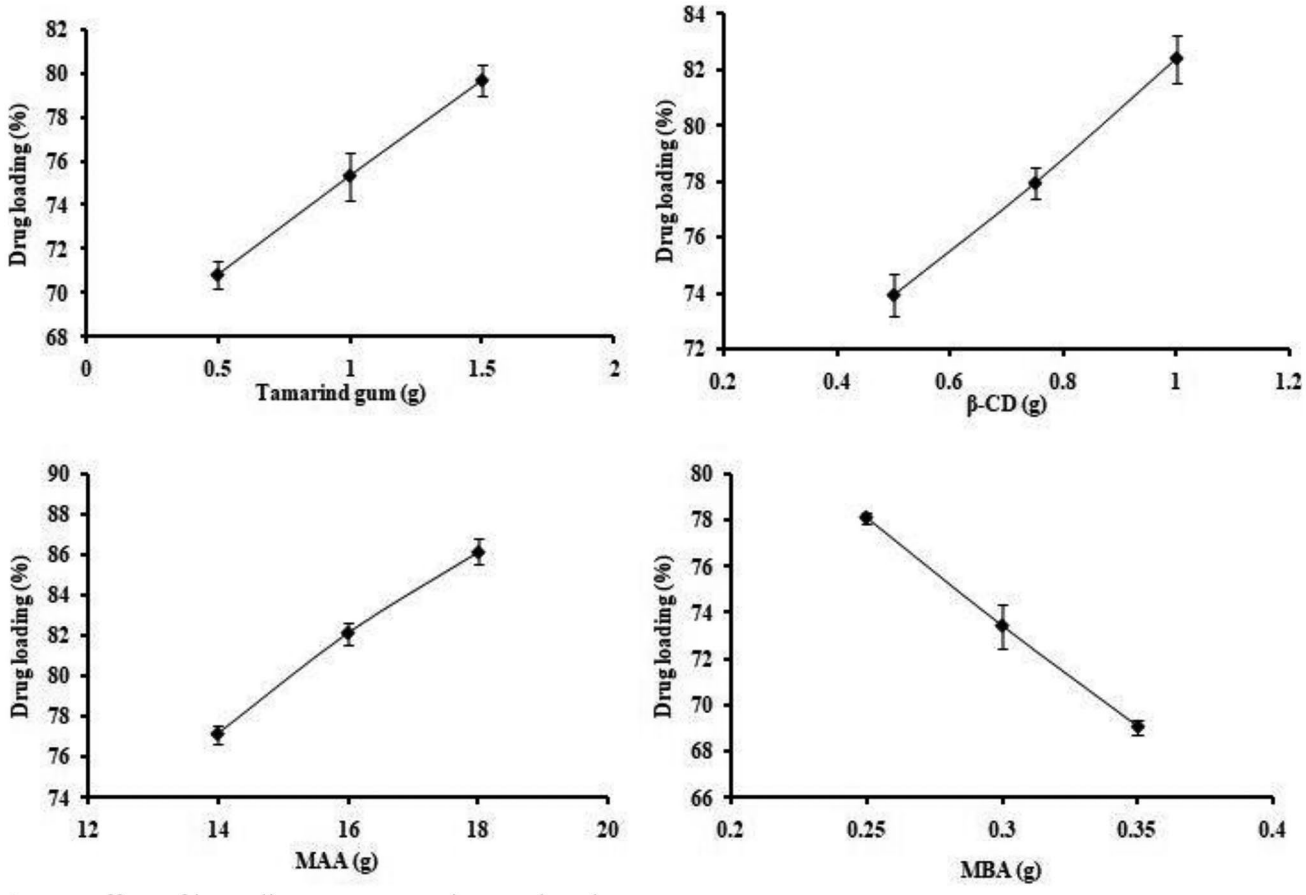

Fig. 2 Effect of ingredients concentration on drug loading

swelling trend (85.03%-95.21%) and that response might be due to availability of greater number of ionizable carboxylic groups from the monomer to graft with polymer backbone causing elongation of the network and excessive uptake of fluid.

Formulations (TGB10-TGB12) with increasing MBA concentrations exhibited decreased swelling trends ranging from 80.44% to 71.38% due to facilitation of polymerization reaction by crosslinker resulting in improved crosslinked density of network and low penetration of physiological fluid.

Optimum results were obtained by formulation TGB9 showing maximum swelling response at pH 7.4.

Sol–gel fraction

Gel fraction of hydrogels was calculated to analyze the consumption of reactants during polymerization reaction. Formulations were developed by varying the ratios of tamarind gum, β-cyclodextrin, MAA and MBA and effect of these components on gel fraction was noticed. All formulations (TGB1-TGB12) exhibited rise in gel fraction ranging from 83.45% to 95.37%. Results are presented in Fig. 4.

Formulations (TGB1-TGB3) having variable amounts of tamarind gum presented increase in gel fraction from 84.06% to 91.49%. Likewise, percentage of gel fraction was promoted from 83.45%-90.41% for formulations TGB4-TGB6 having increasing trends of β-cyclodextrin.

Progressive rise in gel fraction was also noted in formulations (TGB7-TGB9) having methacrylic acid in increasing concentrations that was ranged within 86.80%-93.60%. Elevated gel fraction was due to availability of more carboxylic groups from MAA that promoted polymerization reaction by binding with reactive sites on network structure. Similarly, gel fraction of 87.57%-95.37% was exhibited by formulations (TGB10-TGB12) containing increasing contents of MBA. That effect may be attributed to facilitation of higher polymerization by crosslinking agent giving rise to improvement in crosslinking density of the grafted network.

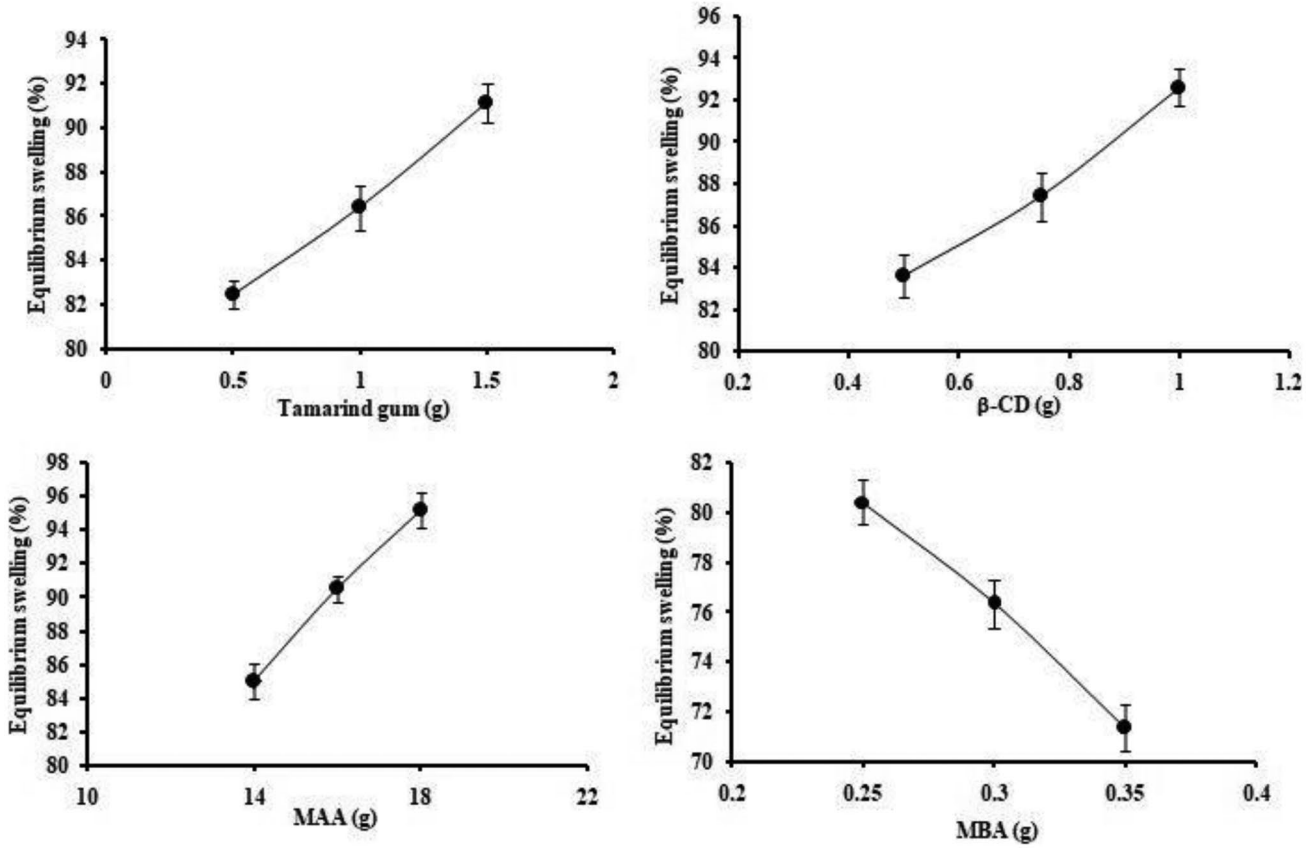

Fig. 3 Effect of ingredients concentration on equilibrium swelling

FTIR analysis

FTIR spectra of Capecitabine, β-CD, tamarind gum, physical mixture and hydrogels were recorded to ensure the compatibility and complexation of components. Spectra of all components are displayed in Fig. 5. IR Spectrum of capecitabine presented evident peaks at 1035.13 cm^{-1} (C-F stretching vibrations), 1240 cm^{-1} (tetrahydrofuran ring), 1650.15 cm^{-1}(pyrimidine carbonyl stretching vibrations), 1697.20 cm^{-1} and 1720.11 cm^{-1} (urethane carbonyl stretching vibrations), 3100.21 cm^{-1} (N–H stretching) and 3300 cm^{-1} (O–H stretching vibrations).

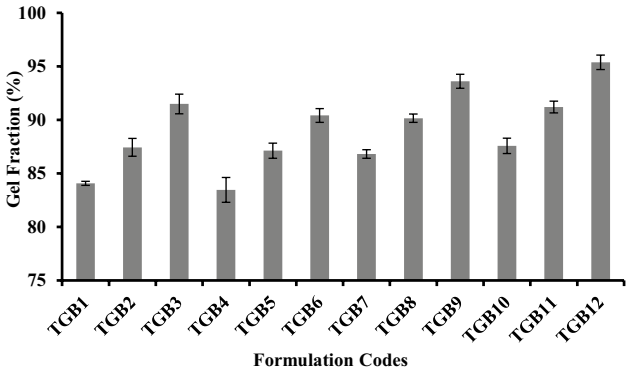

Fig. 4 Gel fraction (%) of formulations TGB1-TGB12

IR Spectrum of β-CD has displayed a transmittance peak at 3244.27 cm^{-1} that corresponded to stretching vibrations of -OH group. A broad peak recorded at 2916.37 cm^{-1} was showing -CH asymmetric stretching vibrations. Other evident peaks appearing at 1666.85 cm^{-1}, 1134.14 cm^{-1} and 1029.99 cm^{-1} were indicating C-O stretching vibrations, C–O–C coupling of glucose and cyclodextrin rings, respectively. Tamarind gum presented broad peaks at 2893.22 cm^{-1} and 1433.11 cm^{-1} corresponding to aliphatic –CH stretching vibrations while characteristic band at 704.02 cm^{-1} was assigned to aromatic –CH group on FTIR spectrum. Moreover, peaks displayed at 1126.43 cm^{-1}. 1060.85 cm^{-1}, 916.19 cm^{-1} and 815.89 cm^{-1} were indicating the presence of xyloglucan (essential constituent of tamarind gum) and attributed to asymmetric stretching of O-C-O, C–C stretching, xyloglucan ring vibration and C-H stretching associated with glucose and xylose, respectively [41].

The FTIR spectrum of tamarind/β-CD-g-poly (MAA) network system displayed the prominent peaks of pure β-CD and tamarind gum with slight displacement and variation in their intensities thus proving the fabrication of new grafted network.

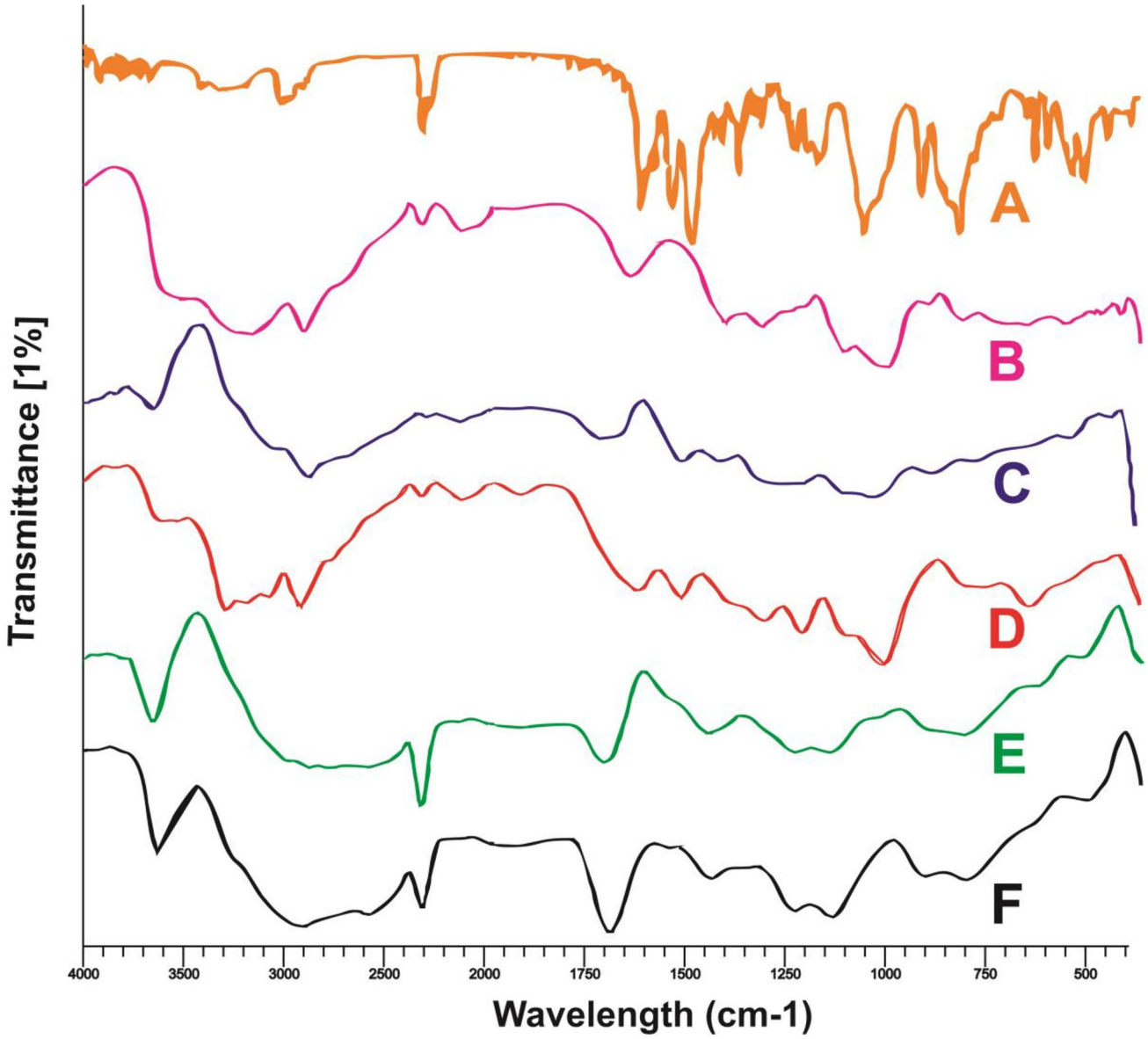

Fig. 5 FTIR spectra of **A** capecitabine **B** β-CD **C** tamarind gum **D** physical mixture **E** unloaded and **F** drug loaded hydrogels

In case of drug loaded hydrogels, certain peaks of tamarind gum appearing at 916.19 cm^{-1} and 815.89 cm^{-1} due to xyloglucan ring and C-H stretching of glucose and xylose were shifted towards higher wave numbers i.e. 939.33 cm^{-1} and 839.03 cm^{-1} indicating the grafting of polymer with other reaction contents. Transmittance peaks of Capecitabine were also visible along with the peaks of other components. Evident peaks of pure Capecitabine appeared at 1240 cm^{-1} and 1720.11 cm^{-1} due to tetrahydrofuran ring and carbonyl stretching vibrations were shifted to 1259.52 cm^{-1} and 1710.86 cm^{-1}, respectively on IR spectrum of drug loaded grafted network suggesting the successful entrapment of Capecitabine within the network (Fig. 5).

Scanning electron microscopy

Grafted tamarind/β-CD-g-poly (MAA) network was evaluated for surface morphology by carrying out scanning electron microscopy. SEM photomicrographs were captured at different magnifications that are displayed in Fig. 6. Smooth and transparent surfaces of hydrogels were visible having glossy appearance. Cracked surface was also evident that might be due to drying of hydrogels. Physiological fluid can easily penetrate through this surface resulting in swelling of hydrogels that governs slow release of Capecitabine from the network system.

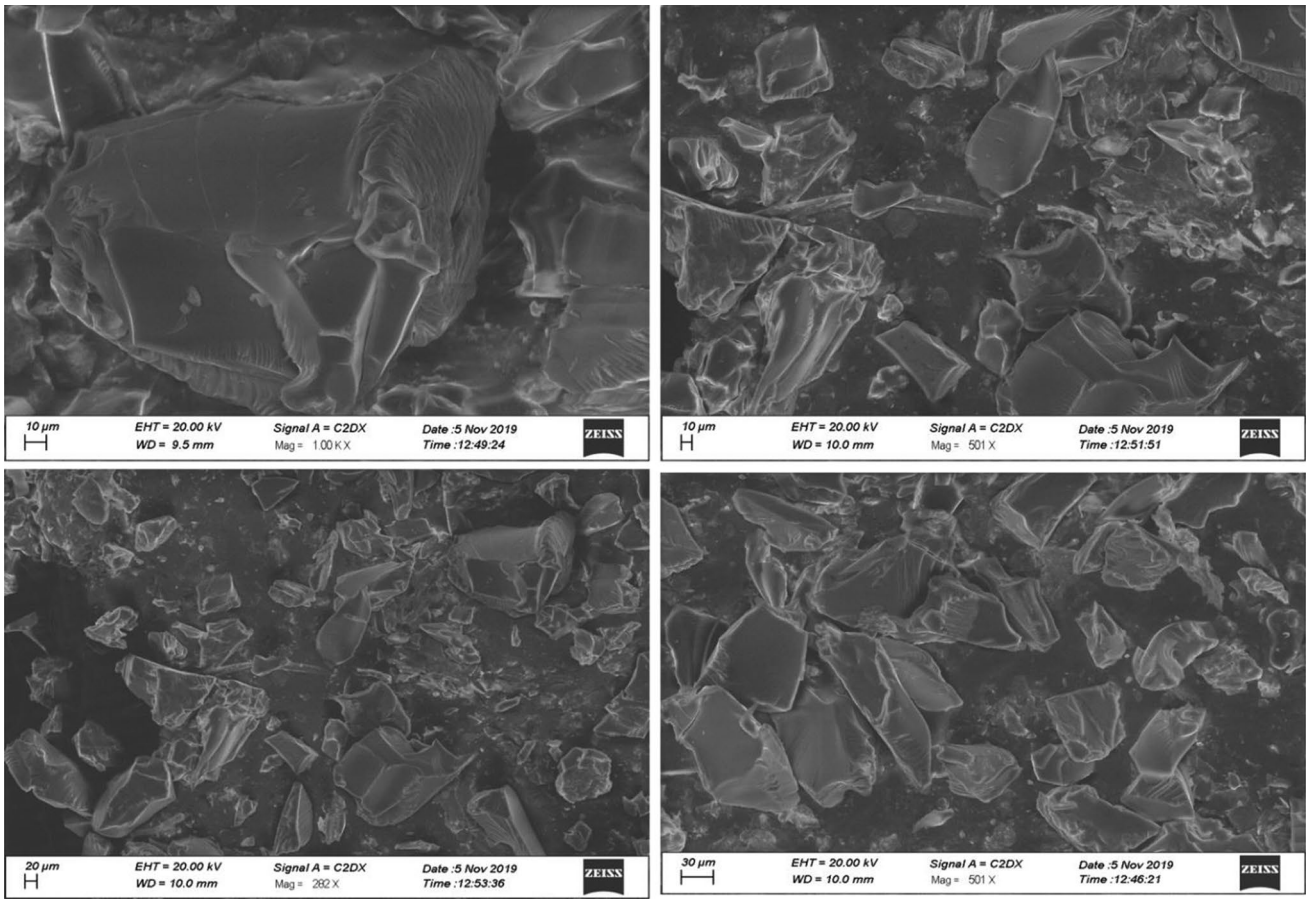

Fig. 6 SEM photomicrographs of tamarind/β-CD-g-poly (MAA) hydrogels at different magnification

Thermal analysis

Pure drug, polymers and grafted network were evaluated by performing DSC and TGA studies. DSC spectra are presented in Fig. 7. DSC thermogram of Capecitabine has presented an endothermic peak at 132.31 °C (0.02265 J/g) that was attributed to the melting point of drug so confirming its crystalline nature. Another peak at 159.70 °C (0.008827 J/g) was due to partial degradation of drug while peak at 456.35 °C (0.0007347 J/g) was attributed to complete combustion of the drug. DSC thermogram of tamarind gum displayed an endothermic peak at 66.62 °C (0.00676 J/g) describing the loss of moisture content. Two other peaks appearing at 305.05 °C (0.02134 J/g) and at 453.21 °C (0.003365 J/g) were assigned to melting of polymer and its chemical degradation, respectively. β-CD thermogram, exhibited prominent endothermic peak at 115.19 °C (0.01958 J/g) attributing to removal of moisture. While endothermic peaks presented at 308.13 °C (0.008759 J/g) revealed melting range of polymer, 350.12 °C (0.009379 J/g) corresponded to degradation of polymer and 423.58 °C (0.006972 J/g) revealing the complete combustion of polymer. Thermogram of drug loaded crosslinked network displayed shifting of Capecitabine, β-CD and tamarind gum peaks towards higher temperatures. Prominent peaks were observed at 69.70 °C (0.09158 J/g), 117.29 °C (0.01055 J/g), 262.54 °C (0.02129 J/g) and 467.56 °C (0.05067 J/g) on DSC spectrum thereby confirming the stability of tamarind/β-CD-g-poly (MAA) hydrogels at elevated temperatures. Mahmood et al. also reported the stability of β -CD based nanocomposite hydrogels at higher temperatures like our findings [42].

TGA thermograms of tamarind gum, β-CD, Capecitabine and drug loaded hydrogels were recorded at temperature range of 0–600 °C as displayed in Fig. 8. TGA spectrum of Capecitabine presented gradual mass loss events with respect to increase in temperature i.e. 7.76% of weight loss at 134.22 °C, 28.38% at 179.09 °C, 54.27% at 296.39 °C and 76.78% of weight loss was observed at 494.74 °C.

Tamarind gum thermogram has shown four stages of mass loss at variable temperatures. Initially, 8.46% mass loss was observed at 101.60 °C that was increased to 14.59% of loss in mass at 288.57 °C. Next degradation step was shown at 349.00 °C presenting 57.74% of mass

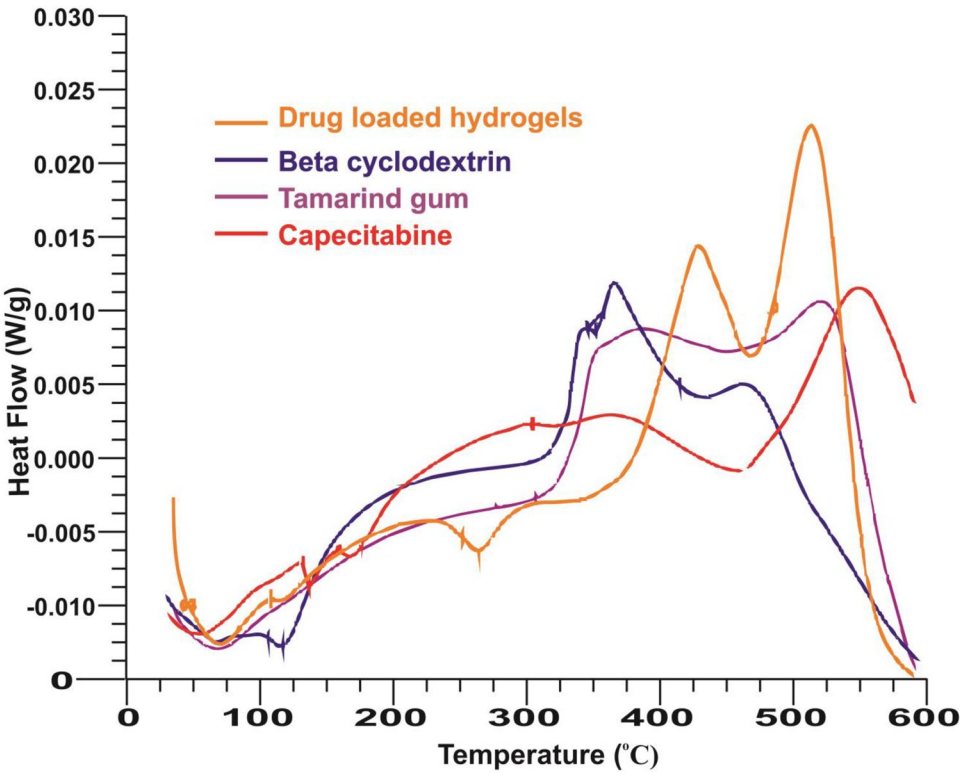

Fig. 7 DSC analysis of capecitabine, tamarind gum, β-CD and drug loaded hydrogels

loss that was increased to 92.55% at 535.26 °C displaying final degradation of the polymer. TGA spectrum of β-CD revealed 2.79% and 25.35% of mass losses at temperatures of 51.12 °C and 115.06 °C, respectively describing the removal of water content from the polymer. Next degradation occurred at 321.27 °C presenting 33.32% weight loss and associated with melting point of polymer. Maximum weight loss of 98.237% took place at 360.38 °C depicting the final degradation of β-CD.

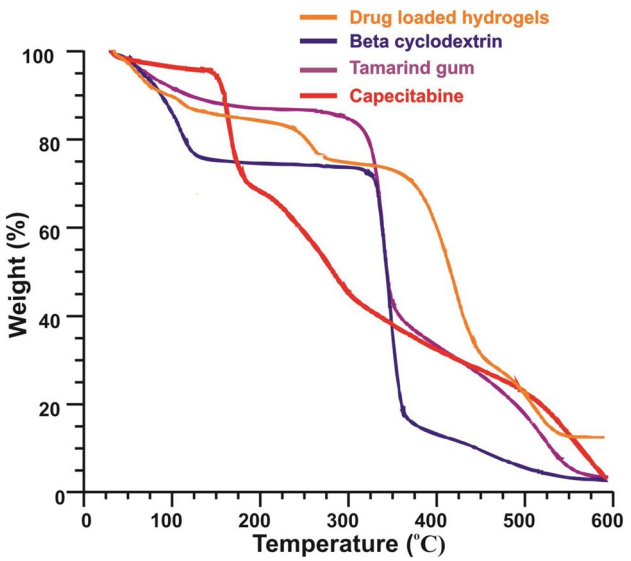

Fig. 8 TGA analysis of capecitabine, tamarind gum, β-CD and drug loaded hydrogels

The spectrum of drug loaded hydrogels showed subsequent mass loss events with respect to rise in temperature. Initial degradation occurred at temperature of 75.30 °C with 9.69% of mass loss then it was raised to 16.51% at 132.17 °C, 21.45% at 238.10 °C, 28.93% at 269.38 °C, 35.48% at 370.33 °C, 79.21% at 441.42 °C and finally 93.75% of mass loss was noticed at 500.43 °C. In case of polymeric network maximum weight loss was observed at higher temperature (above 500 °C) as compared to the individual components thus proving the stability of tamarind/ β-CD -g-poly (MAA) crosslinked structure. Another similar study by researchers also reported the stability of grafted network at elevated temperatures [43].

XRD studies

XRD studies were carried out to verify the crystalline or amorphous nature of tamarind gum, β-CD, Capecitabine and developed network. Diffractograms are presented in Fig. 9. Crystalline nature of Capecitabine was confirmed by the presence of intense peaks at 2θ = 10.75°, 18.95°, 19.6°, 20.05°, 21.45°, 22.1°, 25.45° and 28.65°. Diffractogram of tamarind gum displayed evident peaks at 2θ = 20.4°, 23.35°, 24.65°, 28.24°, 30.53° confirming its crystalline character. Crystallinity of β-CD was also proved by existence of sharp and intense peaks at 2θ = 19.22°, 24.84°, 27.15° and 44.68°

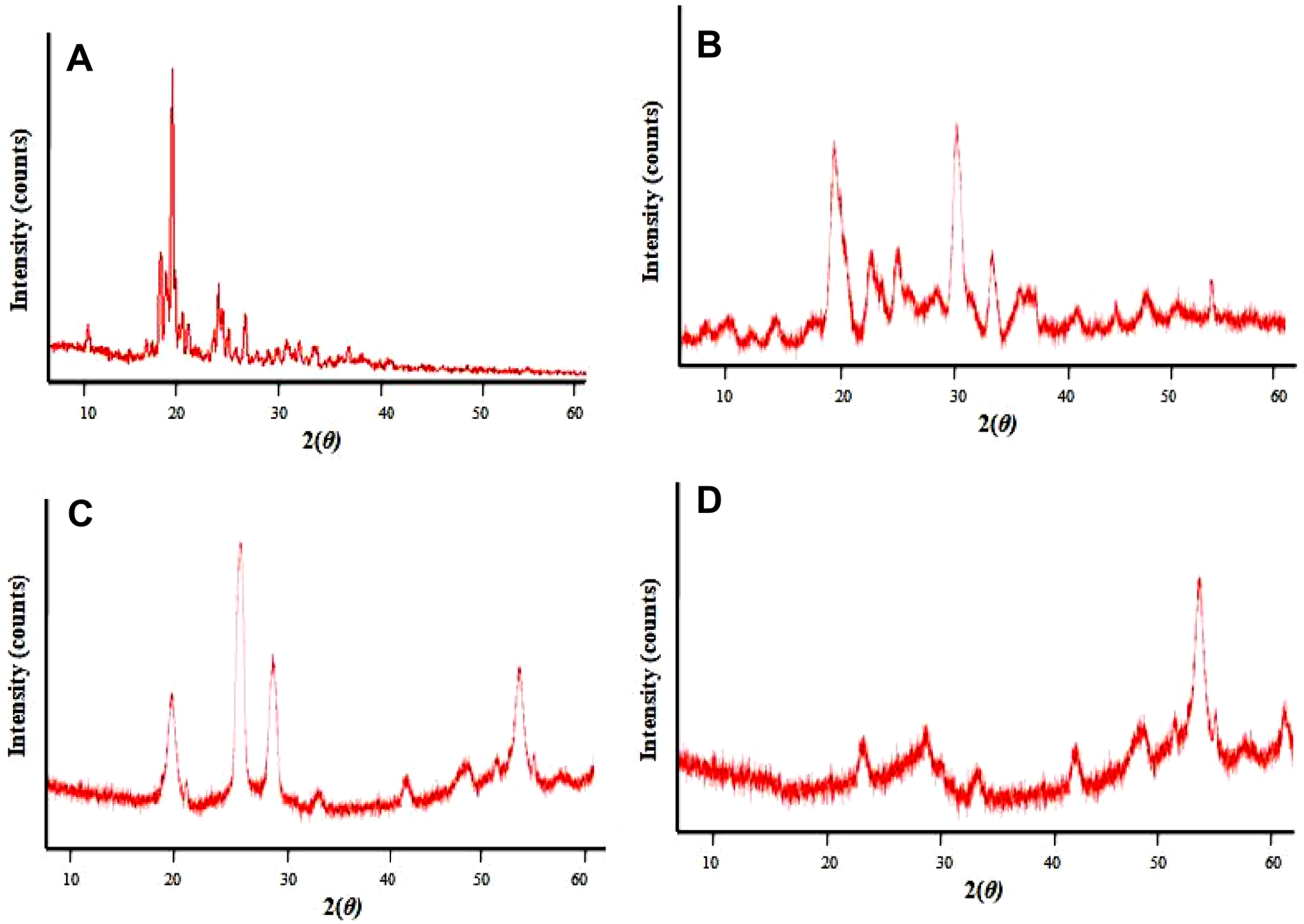

Fig. 9 XRD diffractograms of **A** Capecitabine **B** tamarind gum **C** β-CD and **D** Capecitabine loaded hydrogels

on diffractogram. PXRD studies of developed hydrogels exhibited certain modifications like reduced intensity and height of peaks of polymers and drug. Moreover, certain characteristic peaks of capecitabine were not observed on diffractogram of hydrogels thus supporting the amorphous dispersion of drug within the network system. Conversion of crystalline character of components into amorphous one verified the formation of new grafted polymeric network. Furthermore, amorphous distribution of capecitabine within hydrogels confirms its solubility enhancement. These findings were in agreement with the results reported by Heydari et al. on β-CD based hydrogels of ciprofloxacin [44].

Elemental dispersive spectroscopy

Microanalysis technique, elemental dispersive spectroscopy (EDX) was employed to determine the elemental composition of pure drug, unloaded and drug loaded hydrogels. EDX provides details of elements by calculating the binding energy of electrons in association with atoms having depth of 5–10 mm. Capecitabine, unloaded and loaded hydrogels spectra presented different percentages of elements as presented in Table 3 and Fig. 10. EDX spectrum of unloaded hydrogels showed carbon, nitrogen and oxygen in concentrations of 69.91%, 7.09% and 23.30%, respectively. In case of drug loaded hydrogels these elements were in concentration of 46.56%, 1.11% and 50.93% with addition of fluorine (1.4%) being an essential element of Capecitabine. Existence of fluorine peak and fluctuations in percentages of carbon, oxygen and nitrogen in Capecitabine loaded hydrogels verified the loading of drug within the network system. Quite similar findings were reported previously in a study of dextran hydrogels conducted by Patil et al. [45].

In vitro Capecitabine release studies

Dissolution studies of Capecitabine were carried out at acidic and basic pH to assess the pH dependent release of drug. Effect of different hydrogel contents (tamarind gum, β-CD, MAA and MBA) on rate of drug release was also investigated, results of those are presented in Fig. 11. At pH 1.2 minimal release of Capecitabine was observed i.e.

Table 3 Elemental composition of drug, unloaded and drug loaded tamarind/β-CD-g- poly (MAA) hydrogels

Materials	Elements	Weight %
Capecitabine	C	56.06
	N	10.52
	O	29.54
	F	3.87
Unloaded tamarind/β-CD-g-poly(MAA) hydrogels	C	69.61
	N	7.09
	O	23.30
Loaded tamarind/β-CD-g-poly(MAA) hydrogels	C	46.56
	N	1.11
	O	50.93
	F	1.4

9.676%-14% for all formulations (TGB1-TGB12) while, a remarkable increase in release rate was noticed at pH 7.4 ranging within 72.92% -94.3%.

Formulations comprising of varying feed ratios of tamarind gum (TGB1-TGB3) displayed 72.92% to 85.17% of Capecitabine release. Increase rate of drug release by raising tamarind gum content was due to generation of electrostatic repulsion within functional units of tamarind gum at pH 7.4. This effect resulted in diffusion of excess of dissolution media inside the network giving rise to enhancement of Capecitabine release. Release rate was promoted up to 90.71% for formulations having variable quantities of β-CD (TGB4-TGB6) as presented in figure. Presence of numerous hydroxyl groups in β-CD structure makes this polymer strongly hydrophilic. Availability of these units to graft with carboxylic groups of methacrylic acid causes elongation of the network structure giving rise to penetration of physiological fluid and more release of drug from the grafted network [46].

Similarly with the rise of MAA contents in formulations TGB7-TGB9 Capecitabine release rate was significantly enhanced i.e. 85.27%-94.3% ($p < 0.05$). At basic pH carboxylate anions are produced through deprotonation of carboxylic units of MAA that cause repulsion and expansion within the network. This phenomenon contributes towards higher release of Capecitabine from the hydrogel due to excessive uptake of dissolution media by cross linked structure [44].

Unlike above formulations, decrease in release up to 73% (TGB12) was noticed on increasing the crosslinker (MBA) content and that decline in drug release was attributed to promotion of polymerization reaction by MBA causing increase in cross linking density of the hydrogel. More dense structure retarded the release of drug from network. These impacts of MBA on drug release were also supported previously by pioneer researchers [47].

Release data was processed through DD solver software and different kinetic models were applied to investigate the release pattern of Capecitabine. Coefficient of regression (R^2) value was ranging within 0.7978–0.9975. Based on these values release of Capecitabine was best expressed by zero order kinetics evidencing the sustained release of drug from the grafted network [48]. Exponent value was greater than 0.89 for formulations TGB1, TGB2, TGB4, TGB7, TGB11 and TGB12 hence super case II transport was followed for these formulations. While non-fickian diffusion was shown by TGB3, TGB5, TGB6, TGB8, TGB9 and TGB10 as value of "n" was ranged within 0.785–0.880 for these formulations (Table 4). Optimized formulation was TGB9 showing maximum swelling (%), capecitabine loading and release rate.

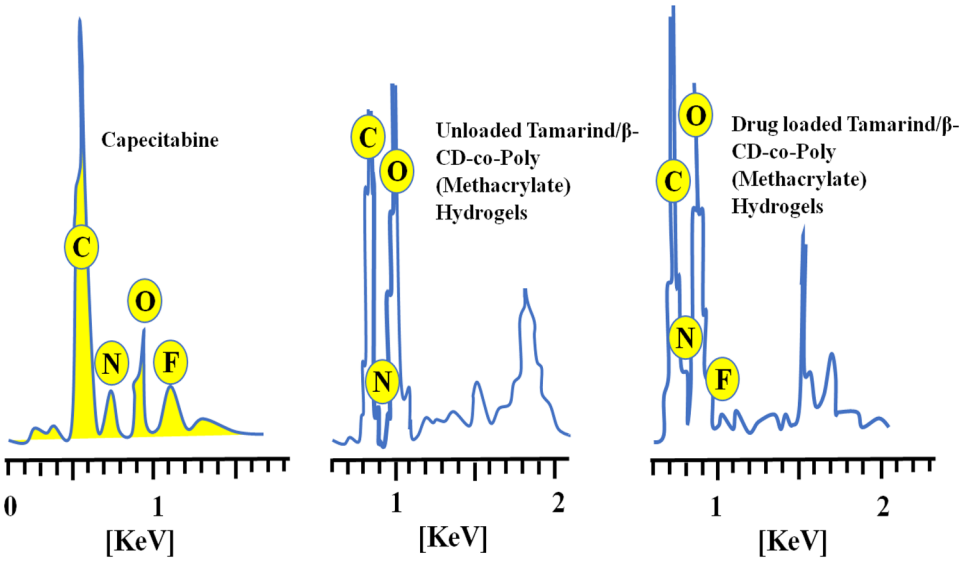

Fig. 10 EDX spectra of drug, unloaded and drug loaded tamarind/ β-CD-g-poly (MAA) hydrogels

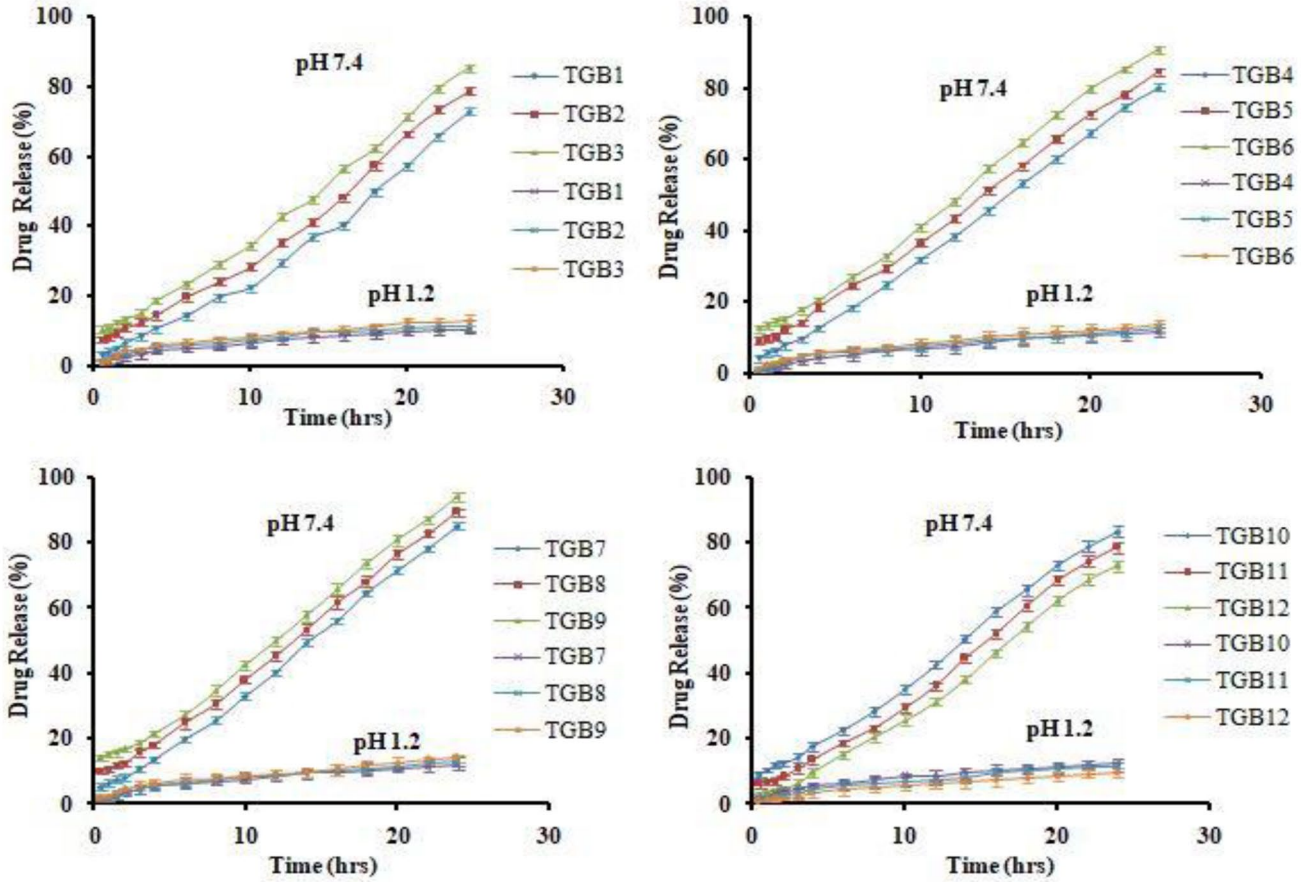

Fig. 11 Capecitabine release profile at pH 1.2 and pH 7.4

Toxicity studies

Toxicity studies were carried out on healthy male rabbits to evaluate the safety of developed tamarind/ β-CD-g-poly (MAA) hydrogels and animals were keenly observed for various parameters like body weight, water and food intake, diarrhea, fever, dermal and ocular toxicity during the study. Both control and tested groups showed no signs of illness. Dermal and ocular toxicities were absent and significant variations were not observed in body weights, water and food consumption of both control and tested groups (Table 5). Hematological and biochemical analysis of blood samples displayed acceptable results as presented in Tables 6 and 7.

Histopathological examination was carried out to investigate the toxicity of developed hydrogels on vital organs of rabbits. On 14th day of study, animals were sacrificed, vital organs were removed and stored in containers having 10% formalin solution. Microscopic evaluation was conducted by preparing H& E stained tissue slides of organs and histological examination was carried out. No signs of lesions, degeneration and other abnormalities were detected in tissues of vital organs of both groups (control and tested) as presented in Fig. 12. Microscopic evaluation of brain presented clear cortical regions, normal axons revealing no sign of inflammatory cell infiltration and cellular

Table 4 Results of kinetic modeling on Capecitabine release data

Formulation	Zero order	1st order	Higuchi	Korsmeyer Peppas	
	R^2	R^2	R^2	R^2	n
TGB1	0.9818	0.9320	0.7978	0.9910	1.201
TGB2	0.9806	0.9368	0.8439	0.9792	1.007
TGB3	0.9725	0.9433	0.8835	0.9780	0.869
TGB4	0.9972	0.9546	0.8430	0.9975	1.03
TGB5	0.9818	0.9613	0.8942	0.9897	0.860
TGB6	0.9644	0.9466	0.9056	0.9814	0.805
TGB7	0.9960	0.9471	0.8445	0.9960	1.029
TGB8	0.9815	0.9494	0.8870	0.9870	0.876
TGB9	0.9552	0.9367	0.9082	0.9763	0.785
TGB10	0.9804	0.9536	0.8843	0.9853	0.880
TGB11	0.9914	0.9456	0.8377	0.9915	1.045
TGB12	0.9890	0.9401	0.8013	0.9974	1.179

Table 5 Clinical findings during acute oral toxicity studies

Observations	Group A (Control)	Group B (Treated)
Signs of illness	Not observed	Not observed
Body weight (Kg)		
Pretreatment	1.90 ± 0.06	1.89 ± 0.05
Day 1	1.90 ± 0.04	1.89 ± 0.06
Day 7	1.91 ± 0.03	1.91 ± 0.04
Day 14	1.93 ± 0.02	1.94 ± 0.03
Water intake (ml)		
Pretreatment	170.30 ± 1.34	165.45 ± 0.85
Day 1	175.55 ± 2.25	170.33 ± 1.65
Day 7	180.40 ± 2.65	190.55 ± 2.57
Day 14	210.33 ± 3.75	215.50 ± 2.35
Food intake (g)		
Pretreatment	69.65 ± 1.70	72.78 ± 1.56
Day 1	70.35 ± 1.50	71.44 ± 1.35
Day 7	74.55 ± 1.32	74.82 ± 1.23
Day 14	73.64 ± 1.06	74.56 ± 1.54
Dermal toxicity	Not seen	Not seen
Ocular toxicity	Absent	Absent
Mortality	Nil	Nil

degeneration. Normal cardiac tissues were observed having specific and precise pattern of cardiomyocytes. There was no evidence of myocardial infarction and hypertrophic cells. Lung tissues of both groups displayed pulmonary oedema, emphysema and alveolar accumulation but lung fibrosis was not noticed. Slight hyperplasia and inflammatory cells accumulation were seen in the portal triad region of liver section. But these abnormalities were not considered to be the result of developed network system as liver and lung sections of control group also presented these changes. Moreover, photomicrographs of kidneys revealed intact bowman capsule, glomerulus and tubules without any damage in both groups. Intestinal tissues of rabbits were having normal muscularis and columnar epithelium without any injury or inflammation. Furthermore, microscopic evaluation of spleen displayed white and red pulp and uniformly distributed white blood cells were observed in the white pulp. No significant difference was noticed in the control group and group treated with tamarind/ β-CD-g-poly (MAA) hydrogels thus providing the safety evidence of polymeric network. Abdullah et al. also reported the non-toxicity of hydrogels by carrying acute oral toxicity studies in healthy rabbits [49].

Table 7 Kidney, liver, and lipid profiles

Biochemical analysis	Group A (Control)	Group B (Treated)
ALT (IU/L)	140.124 ± 2.12	145.40 ± 1.63
AST (IU/L)	32.75 ± 1.52	41.34 ± 2.11
Urea (mmol/L)	13.45 ± 0.61	15.62 ± 2.14
Creatinine (mg/dL)	1.24 ± 0.50	1.19 ± 0.74
Uric acid (mg/dL)	3.72 ± 0.47	3.95 ± 1.25
Cholesterol (mg/dL)	60.35 ± 2.51	59.35 ± 1.60
Triglycerides (mg/dL)	60.62 ± 1.36	55.41 ± 2.25

In-vivo pharmacokinetic analysis of capecitabine

The plasma concentration of capecitabine was calculated to investigate the sustained release character of capecitabine by conducting in-vivo studies in healthy rabbits. For this, oral powder of drug and optimized hydrogel formulation (TGB9) were administered at equivalent doses (10 mg/Kg) to group B and C of animals, respectively. At predetermined time intervals drug concentrations in plasma were detected. Results of comparison of capecitabine plasma profile (pure drug and hydrogel formulation) and pharmacokinetic

Table 6 Results of hematological analysis of rabbits' blood

Parameters	Group A (Control)	Group B (Treated)
Hemoglobin (g/dl)	12.35	11.90
pH	7.25 ± 0.14	7.08 ± 0.26
White blood cells ($\times 10^9 L^{-1}$)	5.2 ± 0.51	7.31 ± 0.33
Red blood cells ($\times 10^6$/ µl)	4.82 ± 2.24	5.10 ± 1.44
Platelets ($\times 10^9 L^{-1}$)	4.58 ± 0.21	5.01 ± 0.12
Monocytes (%)	3.76 ± 0.52	3.56 ± 0.51
Neutrophils (%)	49.84 ± 3.08	53.24 ± 1.66
Lymphocytes (%)	46.37 ± 3.42	41.85 ± 1.87
Mean corpuscular volume (%)	62.75 ± 3.11	68.35 ± 2.54
Mean corpuscular hemoglobin (pg/cell)	22.72 ± 0.61	25.40 ± 1.47
Mean corpuscular hemoglobin conc. (%)	31.60 ± 1.22	35.10 ± 2.50

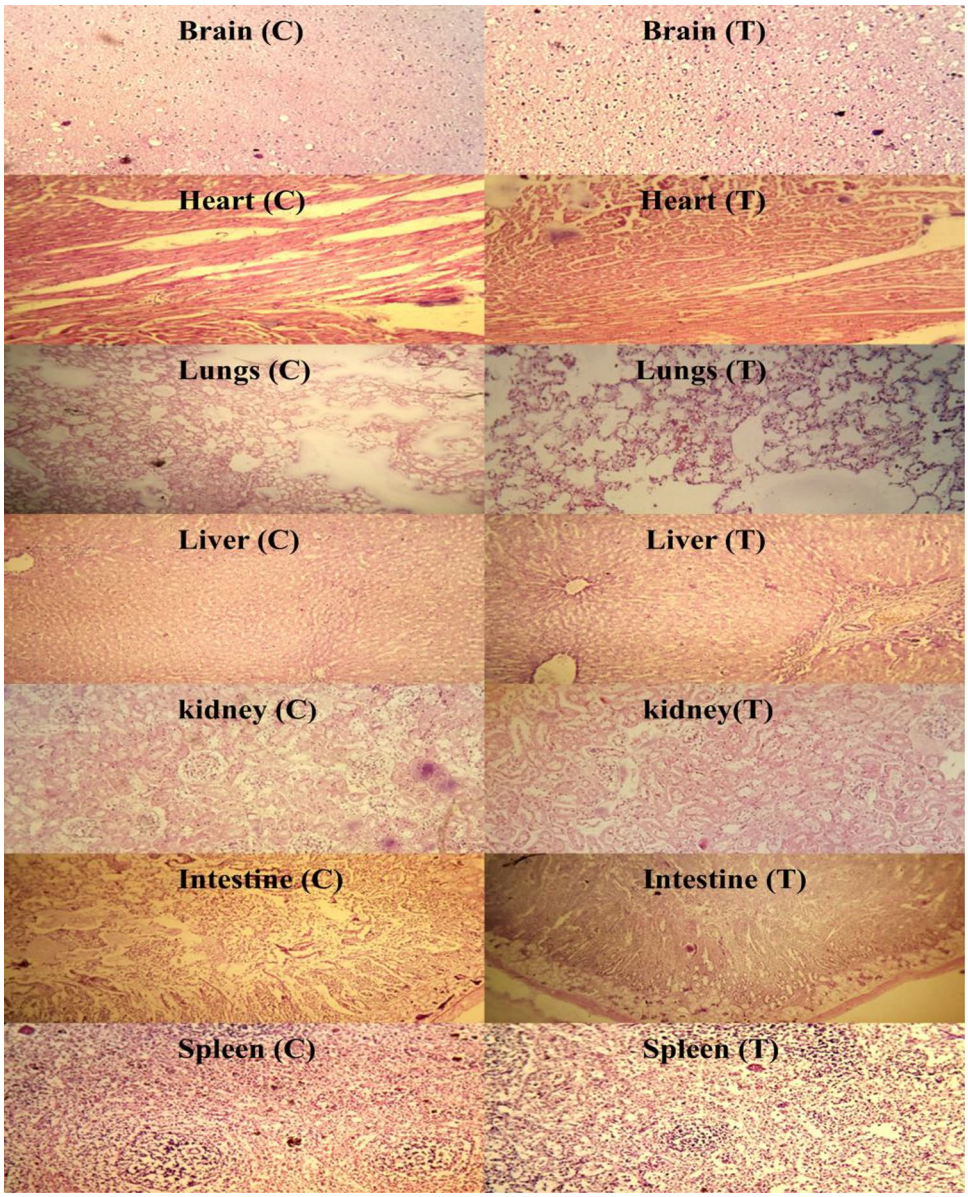

Fig. 12 Histopathological examination of rabbit's vital organs

parameters are presented in Fig. 13 and Table 8. In case of oral powder, maximum concentration of capecitabine (C_{max}) was noted to be 4.44 µg/ml achieved within 2 h (t_{max}) due to rapid absorption of drug. For hydrogel formulation these parameters were found to be 3.58 µg/ml and 3 h, respectively. Half-life of drug was 1.27 h that was prolonged to 14.02 h when administered as tamarind gum/β-CD-g-poly (MAA) hydrogels. That extended half-life can be explained in terms of slow release of capecitabine from polymeric matrix resulting in its sustained effect in plasma and increase in bioavailability. Moreover, a significant difference was also revealed within other pharmacokinetic parameters in case of pure drug and crosslinked network i.e. MRT of pure drug (3.02 h) was prolonged to 16.44 h and AUC was extended

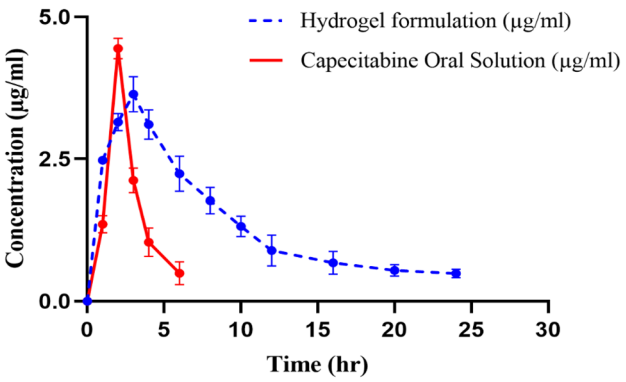

Fig. 13 Plasma concentration vs. time profile of Capecitabine after administration of oral powder and hydrogels

Table 8 Pharmacokinetic parameters of pure Capecitabine and drug loaded polymeric network

Formulations	pK parameters					
	C_{max} (µg/ml)	t_{max}(h)	$t_{1/2}$ (h)	$AUC_{0-\infty}$ (µg.h/ml)	Vd	MRT (h)
Capecitabine oral powder	4.44	2	1.27	10.87	1.68	3.02
Drug loaded hydrogels	3.58	3	14.02	42.43	4.76	16.44

from10.87 µg.h/ml to 42.43 µg.h/ml. Similar trends of differences in C_{max}, AUC and MRT of capecitabine were noticed by previous studies due to slow release of drug from the formulations [50]. Hence, tamarind gum/β-CD-g-poly (MAA) network system proved to be a suitable and efficient platform for delivering and prolonging the release of capecitabine and other chemotherapeutic agents as confirmed by in-vivo studies.

Conclusions

A smart pH responsive tamarind/β-D-g-poly (MAA) network system was successfully developed and loaded with capecitabine for its controlled delivery. The fabricated hydrogels were characterized for structural and compositional characteristics, drug loading percentage, swelling response, thermal stability, elemental analysis, morphology and drug release kinetics. Compatibility and Complexation within the components of hydrogels were confirmed by FTIR and XRD analysis. The pH responsive character was revealed by all formulations as significantly higher swelling and drug release were observed at alkaline pH compared with acidic one. Optimum results were exhibited by formulation TGB9 showing highest drug loading, swelling and capecitabine release. Optimized formulation was further tested for safety profile by carrying oral toxicity studies in healthy rabbits showing no ocular and dermal toxicity, pathological change in blood and other abnormalities. Moreover, in-vivo experiments were also conducted in animals and pharmacokinetic studies displayed the prolonged half-life, AUC and MRT of capecitabine after administration of tamarind/β-CD-g-poly (MAA) hydrogels. So, the developed carrier system exhibited an excellent potential for delivery of capecitabine and other drugs at controlled rate.

Limitations of the study

The limitations of this work include repetitive washing of the hydrogel discs to remove unreactive species is a time consuming process, drug loading and in-vivo estimation of Capecitabine are also timing consuming and expertise demanding parameters.

Acknowledgements The authors would like to sincerely acknowledge the "University of Sargodha and The University of Lahore, Lahore, Pakistan" for providing instrumental support in executing the present research project.

Data availability The authors confirm that the data supporting the findings of this research are available within the article.

Declarations

Competing interest The authors declare that they have no conflict of interest.

References

1. Li J, Mooney DJ (2016) Designing hydrogels for controlled drug delivery. Nat Rev Mater 1(12):1–17
2. Soni G, Yadav KS (2016) Nanogels as potential nanomedicine carrier for treatment of cancer: A mini review of the state of the art. Saudi Pharmaceutical Journal 24(2):133–139
3. Bhattarai N, Gunn J, Zhang M (2010) Chitosan-based hydrogels for controlled, localized drug delivery. Adv Drug Deliv Rev 62(1):83–99
4. Sharpe LA, Daily AM, Horava SD, Peppas NA (2014) Therapeutic applications of hydrogels in oral drug delivery. Expert Opin Drug Deliv 11(6):901–915
5. Mishra B, Upadhyay M, Reddy Adena S, Vasant B, Muthu M (2017) Hydrogels: an introduction to a controlled drug delivery device, synthesis and application in drug delivery and tissue engineering. Austin J Biomed Eng 4(1):1037–1049
6. Lu Y, Sturek M, Park K (2014) Microparticles produced by the hydrogel template method for sustained drug delivery. Int J Pharm 461(1–2):258–269
7. Afshar M, Dini G, Vaezifar S, Mehdikhani M, Movahedi B (2020) Preparation and characterization of sodium alginate/polyvinyl alcohol hydrogel containing drug-loaded chitosan nanoparticles as a drug delivery system. J Drug Deliv Sci Technol 56:101530
8. Pakizeh M, May P, Matthias M, Ulbricht M (2020) Preparation and characterization of polyzwitterionic hydrogel coated polyamide-based mixed matrix membrane for heavy metal ions removal. J Appl Polym Sci 137(48):49595
9. Junior CR, Fernandes RdS, de Moura MR, Aouada FA (2020) On the preparation and physicochemical properties of pH-responsive hydrogel nanocomposite based on poly (acid methacrylic)/laponite RDS. Mater Today Commun 23:100936
10. Jiang Q, Wang J, Tang R, Zhang D, Wang X (2016) Hypromellose succinate-crosslinked chitosan hydrogel films for potential wound dressing. Int J Biol Macromol 91:85–91
11. Shaw GS, Uvanesh K, Gautham S et al (2015) Development and characterization of gelatin-tamarind gum/carboxymethyl tamarind

gum based phase-separated hydrogels: A comparative study. Des Monomers Polym 18(5):434–450
12. Nayak AK, Pal D (2017) Tamarind seed polysaccharide: an emerging excipient for pharmaceutical use. Indian J Pharm Educ Res 51:S136-146
13. Minhas MU, Ahmad M, Khan S, Ali L, Sohail M (2016) Synthesis and characterization of β-cyclodextrin hydrogels: crosslinked polymeric network for targeted delivery of 5-fluorouracil. Drug Deliv 9(10)
14. Malik NS, Ahmad M, Minhas MU (2017) Cross-linked β-cyclodextrin and carboxymethyl cellulose hydrogels for controlled drug delivery of acyclovir. PLoS ONE 12(2):e0172727
15. Abderaman MB, Gueye EH, Dione AN, Diouf AA, Faye O, Beye AC (2018) A molecular dynamics study on the miscibility of polyglycolide with different polymers. Int J Mater Sci Appl 7:126–132
16. Machackova M, Tokarsky J, Capkova P (2013) A simple molecular modeling method for the characterization of polymeric drug carriers. Eur J Pharm Sci 48:316–322
17. Kashirina A, Yao Y, Liu Y, Leng J (2019) Biopolymers as bone substitutes: A review. Biomater Sci 7:3961–3983
18. Meulenaar J, Beijnen JH, Schellens JH, Nuijen B (2013) Slow dissolution behaviour of amorphous capecitabine. Int J Pharm 441(1–2):213–217
19. Agnihotri SA, Aminabhavi TM (2006) Novel interpenetrating network chitosan-poly (ethylene oxide-g-acrylamide) hydrogel microspheres for the controlled release of capecitabine. Int J Pharm 324(2):103–115
20. Taleblou N, Sirousazar M, Hassan ZM, Khaligh SG (2020) Capecitabine-loaded anti-cancer nanocomposite hydrogel drug delivery systems: In vitro and in vivo efficacy against the 4T1 murine breast cancer cells. J Biomater Sci Polym Ed 31:72–92
21. Upadhyay M, Adena SK, Vardhan H, Yadav SK, Mishra B (2018) Development of biopolymers based interpenetrating polymeric network of capecitabine: a drug delivery vehicle to extend the release of the model drug. Int J Biol Macromol 115:907–919
22. Nandi G, Changder A, Ghosh LK (2019) Graft-copolymer of polyacrylamide-tamarind seed gum: Synthesis, characterization and evaluation of flocculating potential in peroral paracetamol suspension. Carbohyd Polym 215:213–225
23. García J, Ruiz-Durántez E, Valderruten N (2017) Interpenetrating polymer networks hydrogels of chitosan and poly (2-hydroxyethyl methacrylate) for controlled release of quetiapine. React Funct Polym 117:52–59
24. Qi X, Li J, Wei W et al (2017) Cationic Salecan-based hydrogels for release of 5-fluorouracil. RSC Adv 7(24):14337–14347
25. Afinjuomo F, Fouladian P, Parikh A, Barclay TG, Song Y, Garg S (2019) Preparation and characterization of oxidized inulin hydrogel for controlled drug delivery. Pharmaceutics 11(7):356
26. Mandal B, Ray SK (2014) Swelling, diffusion, network parameters and adsorption properties of IPN hydrogel of chitosan and acrylic copolymer. Mater Sci Eng C 44:132–143
27. Che Y, Li D, Liu Y et al (2016) Physically cross-linked pH-responsive chitosan-based hydrogels with enhanced mechanical performance for controlled drug delivery. RSC Adv 6(107):106035–106045
28. Chaves LL, Silveri A, Vieira AC et al (2019) pH-responsive chitosan based hydrogels affect the release of dapsone: design, set-up, and physicochemical characterization. Int J Biol Macromol 133:1268–1279
29. Mahmood T, Sarfraz RM, Akram MR, Ismail A, Qaisar MN, Shah PA (2021) Synthesis of CS-g-poly (MAA) nanogels carrier system to improve the solubility of Olmesartan Medoxomil and its in vitro evaluation. Lat Am J Pharm 40:978–990
30. Nesrinne S, Djamel A (2017) Synthesis, characterization and rheological behavior of pH sensitive poly (acrylamide-co-acrylic acid) hydrogels. Arab J Chem 10(4):539–547
31. Punyamoonwongsa P, Klayya S, Sajomsang W, Kunyanee C, Aueviriyavit S (2019) Silk sericin semi-interpenetrating network hydrogels based on PEG-Diacrylate for wound healing treatment. Int J Polym Sci
32. Zou C, Liu Y, Yan X, Qin Y, Wang M, Zhou L (2014) Synthesis of bridged β-cyclodextrin–polyethylene glycol and evaluation of its inhibition performance in oilfield wastewater. Mater Chem Phys 147(3):521–527
33. Pal P, Singh SK, Mishra S, Pandey JP, Sen G (2019) Gum ghatti based hydrogel: Microwave synthesis, characterization, 5-Fluorouracil encapsulation and 'in vitro'drug release evaluation. Carbohyd Polym 222:114979
34. Hassan ZU, Bashir S, Sarfraz RM, Haroon B, Farid B, Mahmood T (2021) Comparative effectiveness of beta-cyclodextrin based copolymeric hydrogel matrices for solubility and bioavailability enhancement of lovastatin: in vitro-in vivo evaluation. LATIN Am J Pharm 40(4):822–833
35. Mo C-E, Chai M-H, Zhang L-P, Ran R-X, Huang Y-P, Liu Z-S (2019) Floating molecularly imprinted polymers based on liquid crystalline and polyhedral oligomeric silsesquioxanes for capecitabine sustained release. Int J Pharm 557:293–303
36. Rana D, Bag K, Bhattacharyya SN, Mandal BM (2000) Miscibility of poly (styrene-co-butyl acrylate) with poly (ethyl methacrylate): Existence of both UCST and LCST. J Polym Sci, Part B: Polym Phys 38:369–375
37. Rana D, Mandal BM, Bhattacharyya SN (1996) Analogue calorimetric studies of blends of poly (vinyl ester) s and polyacrylates. Macromolecules 29:1579–1583
38. Rana D, Mandal BM, Bhattacharyya SN (1996) Analogue calorimetry of polymer blends: poly (styrene-co-acrylonitrile) and poly (phenyl acrylate) or poly (vinyl benzoate). Polymer 37:2439–2443
39. Rana D, Mandal BM, Bhattacharyya SN (1993) Miscibility and phase diagrams of poly (phenyl acrylate) and poly (styrene-co-acrylonitrile) blends. Polymer 34:1454–1459
40. Roy A, Maity PP, Bose A, Dhara S, Pal S (2019) β-Cyclodextrin based pH and thermo-responsive biopolymeric hydrogel as a dual drug carrier. Materials chemistry frontiers 3(3):385–393
41. Alpizar-Reyes E, Carrillo-Navas H, Gallardo-Rivera R, Varela-Guerrero V, Alvarez-Ramirez J, Pérez-Alonso C (2017) Functional properties and physicochemical characteristics of tamarind (Tamarindus indica L.) seed mucilage powder as a novel hydrocolloid. J Food Eng 209:68–75
42. Mahmood A, Amara Sharif FM, Sarfraz RM et al (2019) Development and in vitro evaluation of (β-cyclodextrin-g-methacrylic acid)/Na+-montmorillonite nanocomposite hydrogels for controlled delivery of lovastatin. Int J Nanomed 14:5397
43. Sarfraz RM, Ahmad M, Mahmood A, Akram MR, Abrar A (2017) Development of β-cyclodextrin-based hydrogel microparticles for solubility enhancement of rosuvastatin: an in vitro and in vivo evaluation. Drug Des Dev Ther 11:3083
44. Heydari A, Pardakhti A, Sheibani H (2017) Preparation and characterization of zwitterionic poly (β-cyclodextrin-co-guanidinocitrate) hydrogels for ciprofloxacin controlled release. Macromol Mater Eng 302(6):1600501
45. Patil SB, Inamdar SZ, Reddy KR, Raghu AV, Soni SK, Kulkarni RV (2019) Novel biocompatible poly (acrylamide)-grafted-dextran hydrogels: Synthesis, characterization and biomedical applications. J Microbiol Methods 159:200–210
46. Bartil T, Bounekhel M, Cedric C, Jérôme R (2007) Swelling behavior and release properties of pH-sensitive hydrogels based on methacrylic derivatives. Acta Pharm 57(3):301–314
47. Xu S, Li H, Ding H et al (2019) Allylated chitosan-poly (N-isopropylacrylamide) hydrogel based on a functionalized double network for controlled drug release. Carbohyd Polym 214:8–14

48. Krishnat K, Dhawale SC, Remeth JD, D Havaldar V, Kavitake PR (2017) Interpenetrating networks of carboxymethyl tamarind gum and chitosan for sustained delivery of aceclofenac. Marmara Pharm J 21(4):771–782
49. Abdullah O, Usman Minhas M, Ahmad M, Ahmad S, Barkat K, Ahmad A (2018) Synthesis, optimization, and evaluation of polyvinyl alcohol-based hydrogels as controlled combinatorial drug delivery system for colon cancer. Adv Polym Technol 37(8):3348–3363
50. Kevadiya BD, Chettiar SS, Rajkumar S et al (2014) Evaluation of Montmorillonite/Poly (L-Lactide) microcomposite spheres as ambidextrous reservoirs for controlled release of Capecitabine (Xeloda) and assessment of cell cytotoxic and oxidative stress markers. Compos Sci Technol 90:193–201